Int J Earth Sci (Geol Rundsch) (2009) 98:1691–1703
DOI 10.1007/s00531-008-0319-y

ORIGINAL PAPER

Late Quaternary paleoseismic evidence on the Munébrega half-graben fault (Iberian Range, Spain)

Francisco Gutiérrez · Eulàlia Masana · Álvaro González · Pedro Lucha · Jesús Guerrero · James P. McCalpin

Received: 17 August 2007 / Accepted: 30 December 2007 / Published online: 6 May 2008

Abstract The Munébrega Plio-Quaternary half-graben is a NW-SE trending neotectonic depression located in the central sector of the intraplate Iberian Range (NE Spain). The master fault of the half-graben offsets an Upper Pleistocene pediment deposit, forming an upslope-facing scarp. A trench dug across the fault scarp exposed a 25-m wide deformation zone consisting of graben and horst fault blocks with fissures in the upper part of the scarp, and a monoclinal flexure affected by normal and reverse faults in the lower part of the scarp. We infer a minimum of three faulting events over the past 72 ka, yielding an average (maximum) recurrence interval of 24 ka. The oldest event (72–41 ka) produced an antislope scarp on the relict pediment surface, confining deposition to the downthrown block. Cross-cutting faults affecting sedimentary units deposited in the sediment trap produced by the first event provide evidence for at least two younger events (33–19? ka). The measured cumulative vertical displacement (7.4 m) yield a minimum vertical slip rate of 0.10 ± 0.01 mm/year (2σ error) for the past 72 ka. If the paleoearthquakes ruptured the whole mappable length of the fault (ca. 20 km), they probably had moment magnitudes ca. 6.9 (Stirling et al. Bull Seismol Soc Am, 2002). Such earthquakes would have been more than a magnitude unit larger than the largest ones recorded historically in the Iberian Range. These results suggest that the official seismic hazard assessments, based solely on the historic and instrumental record, may underestimate the seismic hazard in the area.

Keywords Paleoearthquakes · Antislope scarp · Seismic hazard · Extensional tectonics · Iberian Range

F. Gutiérrez (✉) · Á. González · P. Lucha · J. Guerrero
Departamento de Ciencias de la Tierra,
Universidad de Zaragoza, C/Pedro Cerbuna 12,
50009 Zaragoza, Spain
e-mail: fgutier@unizar.es

E. Masana
Departamento de Geodinámica y Geofísica,
Universidad de Barcelona, C/Martí Franqués s/n,
08028 Barcelona, Spain

J. P. McCalpin
GEO-HAZ Consulting Inc, 600 East Galena Ave, P.O. Box 837,
Crestone, CO 81131, USA

Introduction

Predictions on the future spatio-temporal distribution and magnitude of potentially damaging geological processes (e.g., earthquakes, floods, landslides, sinkholes) are commonly based on the extrapolation of their known past behavior. Obviously, the reliability of the forecasts depends largely on the quantity and quality of the available data and on how similar will be the future behavior of the considered process to that in the period of time covered by the analyzed record (Uniformitarianism Law, Cendrero 2003). Generally, extending the record back in time, particularly when dealing with low-frequency (long recurrence interval) processes, allows producing more realistic assessments. In the case of the earthquake hazard, as it has been demonstrated in several areas, the frequently limited reliability of the assessments based solely on historic and instrumental records can be improved by incorporating data on paleoearthquakes and Late Quaternary faults to the hazard analyses (e.g., Reiter 1990, 1995).

Although there is relatively abundant data on Quaternary faults in the Iberian Range (e.g., Gutiérrez et al. 2008), so far, all hazard assessments carried out have relied

only on its low to moderate historical seismicity. Alfaro et al. (1987) proposed a seismotectonic zoning of the Iberian Range taking into account historic earthquakes and the location of some Quaternary faults. However, the available probabilistic seismic hazard analyses (PSHA) consider the whole Iberian Range as a single seismotectonic region and do not take into account the known Quaternary faults. The two most recent PSHAs are the European-Mediterranean Seismic Hazard Map (Jiménez et al. 2001, 2003; Giardini et al. 2003) and the newest official seismic hazard map of Spain, published by the Spanish Government (Ministerio de Fomento 2002, 2003). The former used the seismic zoning for the Iberian Peninsula described by Jiménez et al. (1999). Although the methodology of the latter PSHA remains unpublished, some information about it can be found in García-Mayordomo et al. (2004). In both PSHAs, the seismic activity of each seismotectonic zone was characterized by its Gutenberg–Richter relationship, truncated at the presumably maximum expected earthquake magnitude (M_{max}). For the Iberian Range, the latter was merely based on the historic and instrumental earthquake catalog. The largest historic seismic event in the Iberian Range is the Arnedillo earthquake of 18 March 1817. According to Martínez Solares and Mezcua (2002), it had an estimated moment magnitude of 5.7, and a maximum EMS-98 intensity (European Macroseismic Scale 1998) of VII–VIII. The European-Mediterranean Seismic Hazard Map used $M_{max} = 5.8$ for the Iberian Range (region S24 in Jiménez et al. 1999). Giardini et al. (2003) estimated a peak ground acceleration for a 475-year return period of about $0.08g$ ($g = 9.8$ m/s^2). The official PSHA (Ministerio de Fomento 2002, 2003) reduces this value to less than 0.04 g (less than about intensity VI, EMS-98) for a 500-year return period. The Spanish seismic building code (Ministerio de Fomento 2002, 2003) and the civil protection plan against seismic risk (Ministerio del Interior 2004) are based on this hazard analysis. Because of the low estimated hazard, at present there are officially no requirements for earthquake preparedness or earthquake-resistant building in the Iberian Range.

However, the available information on Quaternary faults (e.g., Baena et al. 1992) and paleoseismic evidence for infrequent but large earthquakes in the Iberian Range ($M_{max} \approx 7$; Gutiérrez et al. 2008) suggests that the official assessments underestimate the earthquake hazard in this intraplate orogen. The primary goal of this research was to check and assess the seismogenic potential of the Munébrega half-graben master fault identified in previous geomorphological maps (del Olmo et al. 1983; Gutiérrez 1996, 1998; Gutiérrez et al. 2008). A trench was dug across an antislope scarp on pediment deposits associated with that fault. This is, to our knowledge, the first trench excavated in the Iberian Range across a Quaternary fault for paleoseismological purposes.

Geological setting and previous work

The NW-SE-trending Munébrega Plio-Quaternary half-graben is located in the central sector of the Iberian Range (Fig. 1). This is an intraplate orogen about 400-km long with a prevailing NW-SE structural grain located in the NE of the Iberian Peninsula. The geomorphology of the Iberian Range is characterized by extensive high-elevation planation surfaces cut across folded pre-Neogene rocks, which are locally interrupted by neotectonic extensional basins (Gutiérrez et al. 2008). The formation of the Iberian Range was initiated in late Cretaceous times by the tectonic inversion of Mesozoic basins (Capote et al. 2002; Sopeña et al. 2004). Shortening in this intraplate setting during the orogenic stage was related to the collision of the Iberian Plate with the European and African plates. In Neogene and Quaternary times (postorogenic stage), the eastern and central sectors of the Iberian Range have been affected by a rifting process generating grabens (Fig. 1) superimposed on the previous compressional structures (Sopeña et al. 2004; Gutiérrez et al. 2008). The normal faults that control the development of these extensional basins result to a great extent from the inversion of inherited basement faults that moved as reverse faults during the Paleogene compression. The origin of these basins, which become progressively younger toward the interior of the Iberian Peninsula (Fig. 1), has been related to the westward propagation of an extensional process that started with the formation of the NE-SW-trending offshore Valencia Trough to the east of the Iberian Range (Anadón and Roca 1996; Capote et al. 2002).

Traditionally, two main phases of postorogenic rifting have been identified in the central sector of the Iberian Range (Capote et al. 2002; Gutiérrez et al. 2008). The first extensional phase, which started in Lower-Middle Miocene times, created the NW-SE-trending Calatayud Graben, and the NNE-SSW-oriented Teruel Graben, both more than 80-km long (Fig. 1). Broadly, these grabens are filled with alluvial fan sediments on the margins that grade into carbonate and evaporite rocks deposited in lacustrine environments in the depocentral sectors. The second extensional phase, developed from the Upper Pliocene to the present day, has created new half-grabens controlled by faults with a prevailing NW-SE trend (Fig. 1), and reactivated the Calatayud and Teruel basins once these had been captured by the external drainage network (Gutiérrez et al. 1996, 2008). The new generation of Plio-Quaternary fault-angle depressions includes the Jiloca Depression and the Daroca and Munébrega half-grabens (Fig. 1).

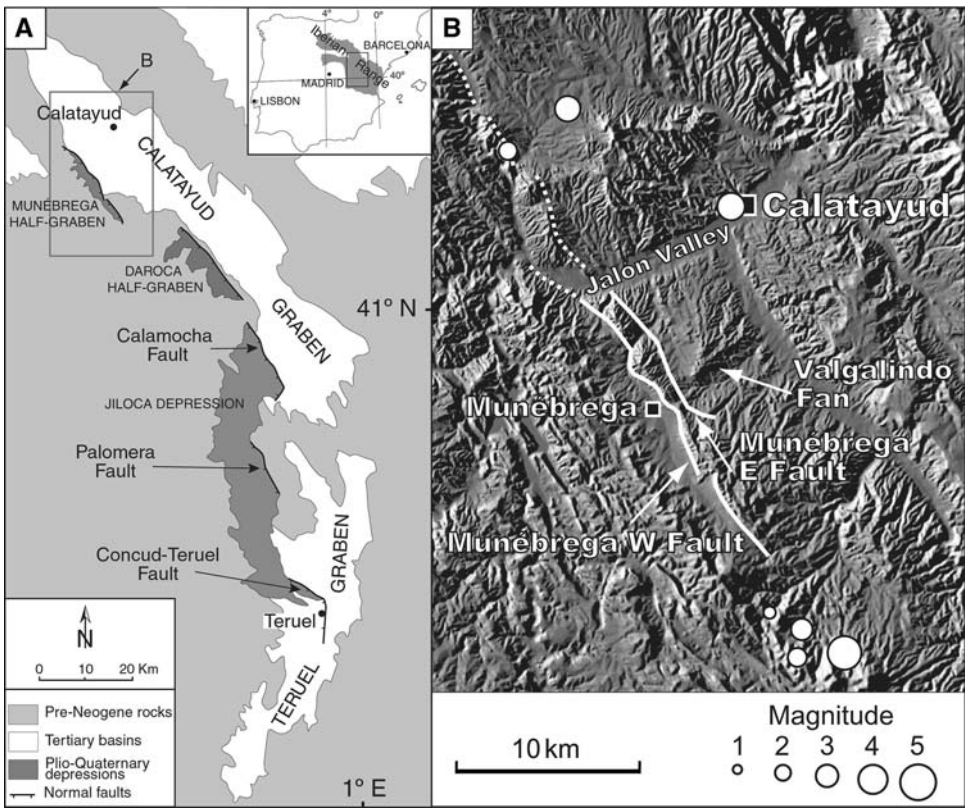

Fig. 1 **a** Geological sketch showing the location of the Tertiary basins and Plio-Quaternary depressions in the central sector of the Iberian Range. **b** Digital elevation model showing the distribution of fault traces, associated lineaments (*dashed lines*) and earthquake epicenters (from data of Table 1)

Numerous works have reported geomorphic and stratigraphic evidence of Quaternary extensional tectonics in these Plio-Quaternary basins. However, in most cases, the timing of the deformation is very poorly constrained due to the lack of geochronological data, hindering the possibility of calculating slip rates for the faults. Moreover, evidence of late Quaternary paleoearthquakes has only been documented in two artificial outcrops in the Jiloca Depression (Burillo et al. 1985; Gutiérrez et al. 2005, 2008). The NNW-SSE-striking Jiloca Depression is a 60-km long half-graben controlled on its eastern margin by three major faults (each 16–24-km long) with a right-stepping *en échelon* arrangement: the Calamocha, Palomera, and Concud-Teruel Faults (Simón 1989; Gutiérrez et al. 2008) (Fig. 1). The Calamocha and Concud-Teruel faults offset Pliocene limestones of the Calatayud and Teruel grabens more than 250 m vertically, yielding a minimum long-term vertical slip rate of 0.05–0.06 mm/year (Gutiérrez et al. 2008). Four coseismic displacement events in the last 72 ka have been inferred from an exposure of Concud Fault, providing an average earthquake recurrence of ca. 18 ka on this structure (Gutiérrez et al. 2005, 2008). On the Palomera Fault it is not possible to calculate vertical offsets due to the lack of correlatable stratigraphic or geomorphic markers on both sides of the structure. Burillo et al. (1985) interpreted two faulting events from two unconformable colluvial units affected by a normal fault located 1.5-km east of the Palomera Fault. According to the archeological dating of the youngest colluvial unit, the displacement events occurred before and after 1,200 B.C., respectively. The NW-SE-trending and ca. 20-km long Daroca Fault controls the Daroca half-graben, which is topographically inset with respect to the Calatayud Graben. The Daroca Fault displaces a mantled pediment that has yielded OSL dates of 119 and 113 ka (Gutiérrez et al. 2005, 2008).

Del Olmo et al. (1983) provided the first account of the Munébrega half-graben in the 1:50,000 scale geological sheet of the area. The 1:100,000 scale geomorphological map included in the report of this sheet depicts the master fault, although it does not represent the rupture of the mantled pediment analyzed in this paper. In a subsequent work, Echeverría (1988) interpreted the Munébrega Depression as a primitive infilled fluvial valley incised along a weakness zone associated with the normal fault that controls the southwestern margin of the Calatayud Graben. Recent works have provided more detailed morpho-structural maps of the Munébrega half-graben revealing the horst structure of the active NE margin and the displacement of a Quaternary mantled pediment along the trace of the basin-bounding fault (Gutiérrez 1996, 1998; Gutiérrez et al. 2008) (Fig. 2). These structures are also depicted in a simplified way in the 1:1,000,000 scale geomorphological map of Spain (Martín-Serrano 2005).

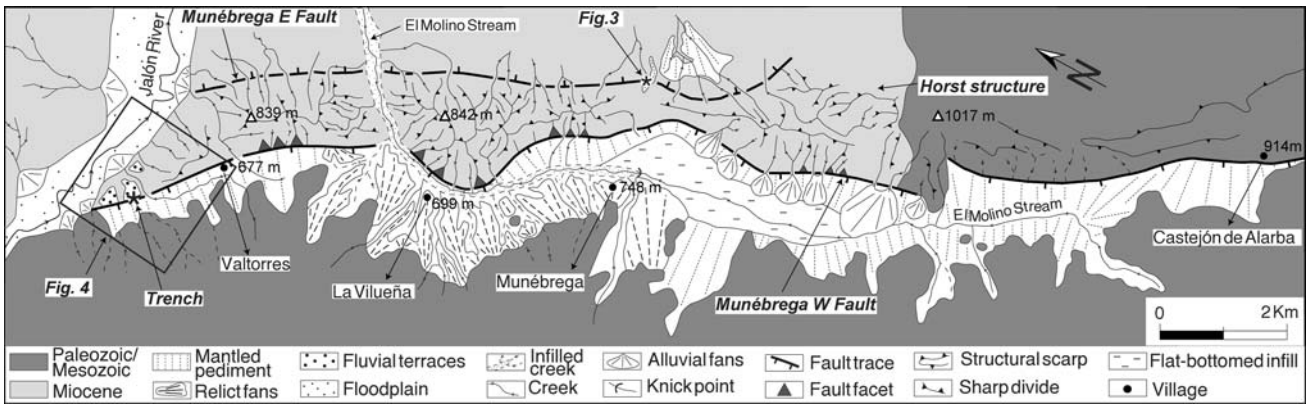

Fig. 2 Geomorphological map of the Munébrega half-graben. *Box* shows the location of Fig. 4

Tectonic geomorphology of the Munébrega half-graben

In the studied sector, the NW-SE-trending Calatayud Neogene Graben is flanked by mountain ranges primarily made up of Paleozoic formations. This basin is traversed perpendicularly by the discordant Jalón River valley, which crosses the basin margins through topographic gaps associated with stepovers of the *en échelon* basin-bounding faults (Gutiérrez et al. 2008) (Fig. 1). The 19-km long Munébrega half-graben is superimposed on and inset into the Calatayud Graben along its southwestern margin, south of the Jalón River valley (Figs. 1, 2). Consequently, the formation of this fault-angle depression started during or after the Lower Pliocene (Gutiérrez 1998), the age of the youngest sediments of the Calatayud Graben basin fill (Adrover et al. 1982).

The active NE margin of the half-graben corresponds to a horst structure flanked by the Munébrega E Fault and the Munébrega W Fault (Fig. 2). The latter is the master fault that controls the development of the basin. The prominent relief of the horst structure, primarily underlain by Miocene conglomerates of the Calatayud Graben fill, was originally attributed to differential erosion favored by a sharp lateral change from conglomeratic facies to less-resistant fine-grained facies (Bomer 1960; Tena and Mandado 1984). However, the topography of this fault block is clearly related to neotectonic uplift in addition to differential erosion favored by the juxtaposition of different facies along the Munébrega E Fault. This interpretation is consistent with the deep dissection of the conglomerates in the horst by high-gradient V-shaped gullies flanked by sharp divides. The smaller size and higher gradient of the drainage basins facing the Munébrega W Fault and the slight topographic asymmetry of the horst may be indicative of a higher slip rate on the Munébrega W Fault (Leeder and Jackson 1993; Burbank and Anderson 2001). About 1 km east of the Munébrega E Fault there is a 4-km long relict alluvial fan (Valgalindo Fan) inset into the Calatayud Graben fill whose apex points to a topographic gap in the horst east of Munébrega village (Fig. 1). The origin of this alluvial fan is most likely related to the tectonic rejuvenation of the horst (Gutiérrez 1998; Gutiérrez et al. 2008).

The surface trace of the NE-dipping Munébrega E Fault is defined by a 10-km long topographic lineament reflected by a conspicuous break in slope (Fig. 2). A 14-km long prolongation of this lineament composed of three segments with a left-stepping arrangement has been mapped north of the Jalón valley (Gutiérrez 1998; Fig. 1). South of the Jalón River, the Munébrega E Fault follows a N155E direction changing progressively into an ESE-WNW strike in its southern sector. This bend seems to be related with a stepover on the Calatayud Graben margin (Fig. 2). Several streams show sharp deflections controlled by the Munébrega E Fault. The fault crops out in a cutting of the C-102 road east of Munébrega (Fig. 3) where it strikes N155E, dips 70°NE, and juxtaposes two Miocene sedimentary units. The footwall sediments consist of tabular beds of pale orange sandstones and pebble-sized conglomerates (sheetflood deposits). The hanging-wall sediments are made up of massive, matrix-supported bouldery cobble conglomerates (debris flow deposits) and massive beds of gray marly shales with scattered gravels. The sediments of the downthrown block are affected by a small keystone graben controlled by a subsidiary antithetic fault and a dense network of subvertical joints. These dilational joints, with secondary carbonate fills 1–3-cm wide, show an average spacing of 20–30 cm and a strike subparallel to the Munébrega E Fault. The faults and the carbonate-filled joints are truncated and unconformably overlain by an undeformed mantled pediment deposit about 2-m thick. A sample collected 20 cm above the unconformity has provided an age of 7,921 ± 587 OSL year BP (error at 1σ), which postdates the most recent displacement event (MRE) on this fault. Although the conspicuous geomorphic expression of this fault suggests that it has been active in Quaternary times, we cannot demonstrate this point. In any

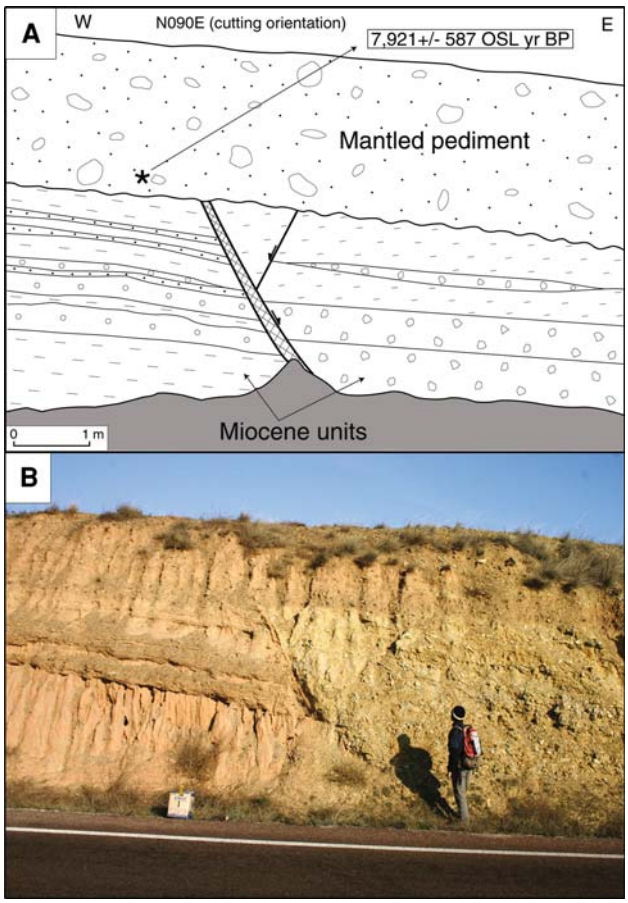

Fig. 3 The Munébrega E Fault exposed in the C-102 road cutting. View is to the north. **a** Sketch of the fault exposure. Miocene units are displaced by the east-dipping fault, but the overlying Holocene (<7.9 ka) pediment deposits are not offset. **b** Photograph of the same exposure

case, it has a fainter geomorphic expression and thus probably a lower activity than the Munébrega W Fault.

The SW-dipping Munébrega W Fault, master fault of the Munébrega half-graben, has a relatively sinuous trace (Fig. 2). Between Munébrega and Castejón de Alarba it shows a small left stepover with a bedrock salient that narrows the basin. The stepover and the salient coincide with a stepover on the Calatayud Graben margin. South of this salient the fault runs parallel to a SW-dipping reverse fault in the upthrown block affecting Paleozoic and Triassic rocks (Del Olmo et al. 1983), suggesting that the Munébrega W Fault may result from the inversion of an Alpine thrust system (Gutiérrez 1998; Gutiérrez et al. 2008). This fault has generated a well-defined mountain front 180-m high with conspicuous triangular facets on Miocene conglomerates (Fig. 2). Faults together with carbonate-filled joints are exposed in the walls of some gullies along the fault trace between Valtorres and Munébrega. However, it is not possible to ascertain whether the downthrown sediments correspond to Miocene conglomerates or indurated Plio-Quaternary deposits. In the northwestern sector of the basin, the Munébrega W Fault has offset a mantled pediment linked to a terrace of the Jalón River, generating a 6–7-m high uphill-facing scarp (Fig. 4, 5). To the northwest, the fault trace gives way to a 4.5-km long lineament defined by a linear stretch in the southern Jalón valley margin and a straight stream that dissects Paleozoic rocks at the northern valley margin (Fig. 1)

The Munébrega Depression was captured sometime in the Quaternary by the El Molino Stream through a water gap located NE of La Vilueña. The piracy of the basin by this transverse drainage induced an incisional wave that propagated along the axis of the basin by headward erosion. The longitudinal profile of the El Molino Stream, entrenched up to 30 m in the basin fill, shows a conspicuous knick point 3 km upstream of the capture area (Fig. 2). The sedimentary fill, more than 30-m thick, is very poorly exposed due to the scarce dissection. In the Munebrega and La Vilueña areas it consists of tabular layers of angular gravels and sands deposited in alluvial fans, mostly by sheetfloods (Blair and McPherson 1994). In this sector the fan surfaces are underlain by a petrocalcic horizon that displays stage V of the carbonate morphological sequence proposed by Machette (1985). The

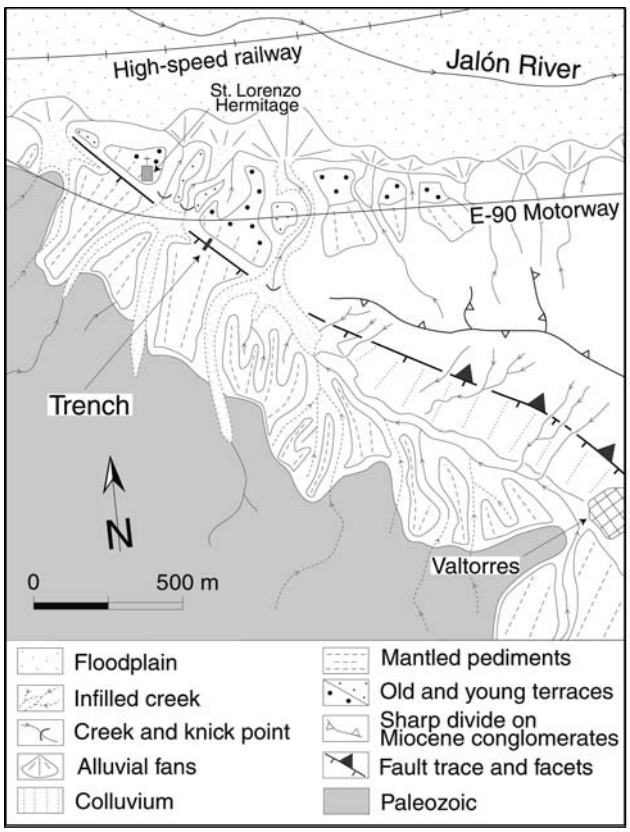

Fig. 4 Detailed geomorphological sketch of the northwestern termination of the Munébrega W Fault and the trench area

Fig. 5 Oblique aerial view of the uphill-facing scarp produced by the Munébrega W Fault and location of the trench

sedimentary infill wedges out rapidly towards the southwest, onlapping the Paleozoic bedrock and forming a highly embayed margin. The limited width of the basin fill is very likely due to the highly irregular topography developed on the Paleozoic rocks previous to the formation of the half-graben. The basin fill is locally interrupted by inliers of Paleozoic bedrock that protrude above alluvial fan surfaces (Fig. 2).

Four different geomorphic domains can be differentiated in the basin, largely conditioned by their position with respect to the capture points and local base levels (Fig. 2). From NW to SE these are: (1) The northwestern sector of the basin shows dissected mantled pediment surfaces whose development has been controlled by the Jalón River. (2) From the knick point of the El Molino Stream to about 2 km northwest of La Vilueña, the basin shows dissected alluvial fan surfaces underlain by resistant Bk horizons. Upstream of the knick point the incision of the El Molino Stream is negligible, probably artificial, and aggradation processes dominate. (3) From the knick point to the bedrock salient the basin displays a relatively flat floor flanked by mantled pediments and debris cones. (4) Southeast of the salient the basin bottom is occupied by mantled pediments that merge along the axial El Molino Stream.

Instrumental seismicity and present-day stress field

The Munébrega normal faults may be spatially associated with contemporary seismicity, and fault orientation is consistent with the present-day stress field. The epicentres of instrumentally recorded earthquakes until November 2007 (catalogue of the Instituto Geográfico Nacional 2007) in the vicinity of the faults are listed in Table 1 and shown on Fig. 1. The location error of these events reaches several kilometers (Instituto Geográfico Nacional 2007), and their focal mechanisms are unknown. Five earthquakes occurred just SE of the mapped trace of the Munébrega W Fault. The largest event of this group is the damaging Used earthquake (Rey-Pastor and Bonelli 1957; Mezcua 1982) of 28 September 1953, (magnitude 4.7, maximum intensity of VII, and hypocentral depth of 15 km; Table 1). The other four events of this group form a small spatio-temporal cluster that occurred in October 2002. They have magnitudes between 1.5 and 2.9 and hypocentral depths between 3 and 13 km. Two more events, with magnitudes of 3.5 and 2.4, and hypocentral depths of 20 and 14 km, respectively, have been recorded close to the extension of the Munébrega E Fault northwest of the Jalón River. The present-day, regional stress field in the Iberian Chain is extensional (Herraiz et al. 2000; Olaiz et al. 2006). In the Munébrega half-graben region, the maximum horizontal stress inferred from focal mechanisms and borehole breakouts is oriented NW-SE to N-S (Herraiz et al. 2000; Andeweg 2002; Jabaloy et al. 2002; Henares et al. 2003; Olaiz et al. 2006), roughly parallel to the traces of the Munébrega Faults. This stress field is consistent with extensional deformation on the NW-SE trending Munébrega faults.

Trenching across the Munébrega W Fault antislope scarp

Geomorphology of the trench site and trenching strategy

As indicated above, in the southern margin of the Jalón River valley and at the northwestern termination of the Munébrega half-graben, the Munébrega W Fault has offset a mantled pediment creating a straight upslope-facing scarp approximately perpendicular to the pediment gradient (Figs. 4, 5). Some meters NE of the fault scarp, the pediment alluvium is interfingered with the deposits of a Jalón River terrace situated at about 45 m above the current channel ("old terrace" on Fig. 4). Based on its relative altitudinal position, an Upper Pleistocene age was expected for this morpho-stratigraphic unit (Gutiérrez 1998). A preliminary description of the deposits was carried out previous to the trench excavation from the scarce available outcrops. The pediment deposits consist primarily of tabular layers of angular, poorly-sorted, monomictic gravels and sands derived from the Paleozoic bedrock of the southwestern margin of the half-graben. The terrace fill, up to 15-m thick, shows typical fluvial facies with polymictic, well-sorted and rounded gravels. A normal fault affecting pediment deposits with an unknown vertical separation was identified in a small outcrop about 200 m east of the trench site.

The fault scarp, which locally acts as a barrier for the surface flow, is traversed by some discordant streams

Table 1 Instrumentally-recorded earthquakes up to November 2007 with epicentres close to the Munébrega Faults (latitude 41.1° to 41.4°, longitude −1.8° to −1.5°). They are plotted in Fig. 1

Date (year/month/day)	Time (hour:minute:second)	Latitude (degrees)	Longitude (degrees)	Depth (km)	Maximum intensity (MSK)	Magnitude (m_{bLg})
1944/02/04	13:21:52	41.35	−1.65		VI	3.8
1944/02/05	12:15:47	41.35	−1.65		III	3.5
1953/09/28	21:41:10	41.13	−1.58	15*	VII	4.7
1981/05/11	10:29:22	41.40	−1.76	20		3.5
2002/10/05	17:57:03	41.14	−1.61	4		2.9
2002/10/05	20:18:30	41.13	−1.61	3		2.5
2002/10/05	20:26:52	41.15	−1.63	13		1.5
2002/10/10	22:05:05	41.13	−1.61	5		2.5
2007/02/24	12:58:01	41.38	−1.80	11		2.4

Data from the Instituto Geográfico Nacional (2007), except the depth of the Used earthquake (asterisk), which was estimated by Samardjieva et al. (1999). Magnitude is in m_{bLg} scale (body-wave magnitude calculated from the *Lg* wave)

(Fig. 4). These streams, especially those located SE of St. Lorenzo Hermitage, show markedly different geomorphic characteristics on opposite sides of the fault trace. The scarcely entrenched valleys developed on the downthrown block change abruptly through conspicuous knick points into incised gullies on the upthrown block. The lower terraces mapped in these valleys, inset with respect to the Jalón River terrace, were produced by these transverse streams. The antislope scarp reaches its largest height west of the St. Lorenzo Hermitage due to the headward erosion caused by a subsequent stream along the toe of the scarp. In the trench area the scarp is 6–7-m high and around 30-m wide, showing a continuous profile with an average slope of 8–9° (Fig. 6). The mantled pediment surface SW of the fault scarp has an average inclination of 3–4°.

The selection of the trench site (41°18′29″N; 1°45′25″W) was determined by the following criteria: (1) The Quaternary offset deposits were expected to be within the dating range of the OSL method (Upper Pleistocene). (2) The mantled pediment deposits contain appropriate sand facies for OSL dating. (3) The vertical offset of the Quaternary deposits was not expected to be very large, so slip rates could be calculated on the basis of dated correlative sedimentary units found on both fault blocks. (4) The antislope scarp creates a trap for sediments where a rather complete late Quaternary paleoseismic record might have been preserved. (5) The slope where the trench was dug was an abandoned vineyard whose owner provided permission.

A single slot trench was excavated on 29 May 2006 perpendicular to the fault scarp with a backhoe. The trench was 40-m long, around 2-m wide and up to 2-m deep (Fig. 6). A reference grid with horizontal and vertical strings spaced 1 m apart was placed on both walls of the trench. The two trench faces were logged with tracing paper mounted on photomosaics produced by joining orthorectified photographs of the grid squares. Key distances between piercing points were measured in the field. The OSL samples were collected by driving PVC tubes into the trench walls, and were analyzed by the Dating Laboratory of the Universidad Autónoma de Madrid, Spain. Environmental background radiation at sample points was measured by personnel of the Laboratory with a scintillation counter of NaI doped with Tl for date correction. The same procedure was followed for the OSL sample from the Munébrega E Fault. Details on these single-aliquot OSL datings are provided in Table 2. The trench was filled a few weeks after the sample collection.

Stratigraphy and geochronology

Four main stratigraphic units have been identified on both walls of the trench: A, B, C and D, following stratigraphic order (Fig. 6). Units A and B are affected by multiple deformational structures, whereas unit D, and very likely unit C, remain undeformed.

The A1 subunit, which extends on both the upthrown and downthrown blocks, corresponds to the top sediments of the mantled pediment previous to the first rupturing event that initiated the development of the antislope fault scarp. It interfingers and overlaps the terrace deposits of the Jalón River terrace located a few meters to the NE. This subunit consists of tabular sheetflood gravel deposits with intercalated sands. The imbricated fabric of the gravels indicates paleocurrents coming from the SW, consistent with the original slope of the mantled pediment. The top of the unit shows a reddish Bt horizon overlain by a calcic horizon that displays the stage II–III of Machette's (1985) morphologic sequence. A sample collected from a sand layer within this unit has yielded an age of 71,809 ± 5,555 OSL years BP (error at 1σ). In the footwall zone, the top of A1 subunit and the soil horizons are truncated by a gravel channel (A2 subunit). The most

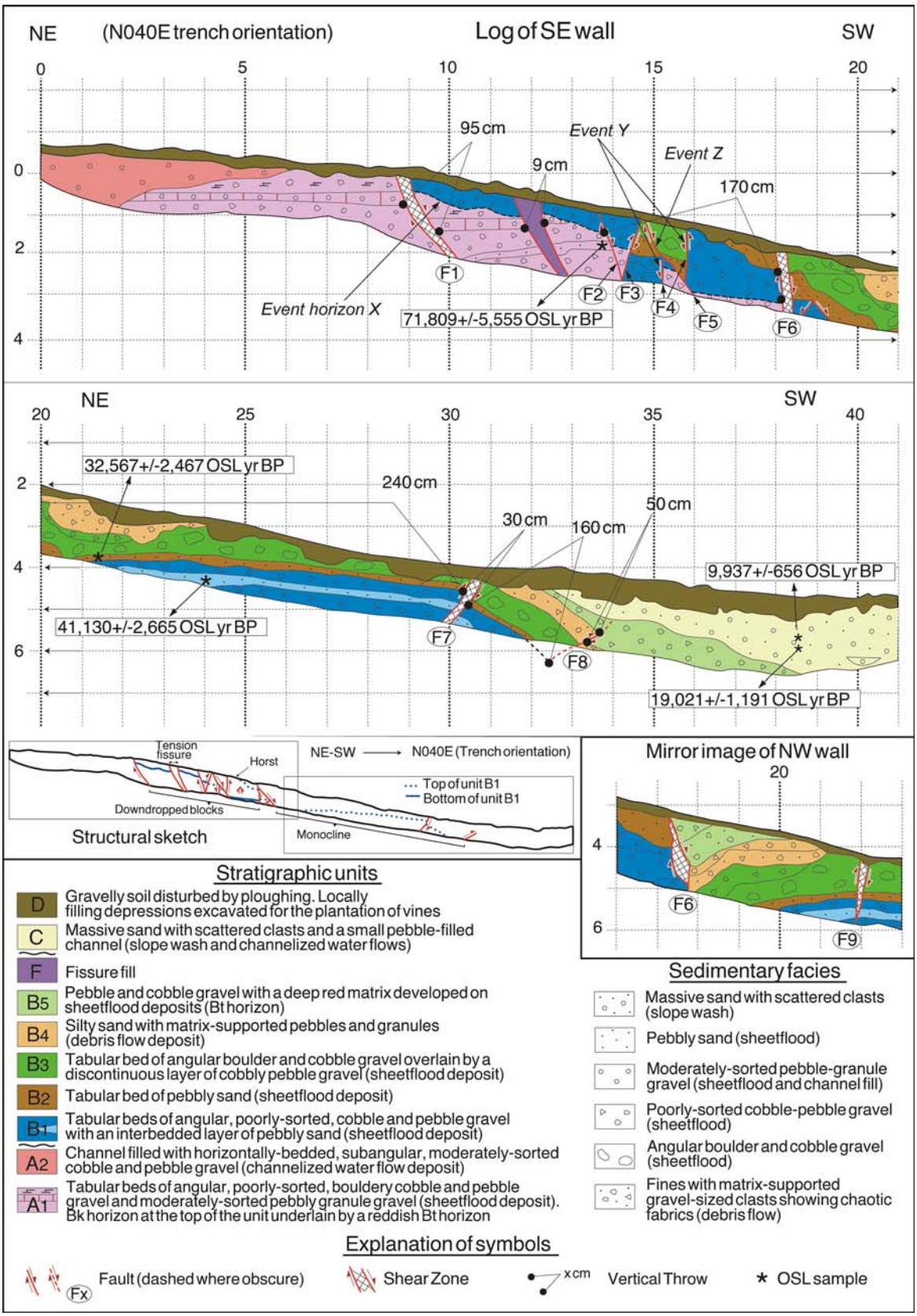

Fig. 6 Log of the SE wall of the trench and partial log of the NW wall. Indicated error range of OSL samples is at 1σ

Table 2 Data on the OSL dates

Sample	Lab code	Equivalent dose (Gy)	Annual dose (mGy/year)	Date (1σ error)	Th (ppm)	U (ppm)	K_2O (%)	H_2O (%)
FMG 4 + 6	MAD-4801	366.23 ± 30.52	5.1	71,809 ± 5,555	27.04	0.001	0.81	2.48
FMG 10	MAD-4746	132.44 ± 6.43	3.22	41,130 ± 2665	17.52	0.001	1.07	0.36
FMG 12	MAD-4803	115.94 ± 10.75	3.56	32,567 ± 2,467	17.55	0.001	0.64	5.82
FMC 15A	MAD-4727	53.26 ± 2.91	2.8	19,021 ± 1,191	12.67	0.001	1.28	1.89
FMC 15B	MAD-4728	39.65 ± 2.6	3.99	9,937 ± 656	20.75	0.001	1.83	1.89
FMEG	MAD-4858R	27.33 ± 2.35	3.45	7,921 ± 587	0.29	5.75	2.16	20.7

reasonable interpretation is that this paleochannel was formed before the footwall relict surface became disconnected from the rest of the pediment by the formation of an uphill-facing scarp.

Unit B, with an exposed thickness of around 5 m, is restricted to the SW of fault F1 (Fig. 6). It consists of gravel facies with sand intercalations deposited by sporadic sheetfloods and debris flows produced by severe rainfall events. The clast imbrication also indicates paleocurrents coming from the SW. A more detailed description of the subunits is provided in Fig. 6. Samples collected from B1 and B2 subunits have been dated by OSL at 41,130 ± 2,665 and 32,567 ± 2,467 years BP (errors at 1σ). The base of B1 subunit shows an unconformable contact over A1 subunit between stations 9 and 14. On the other hand, the subunits B1–B4 become thicker and less tabular to the SW. The highest preserved thickness of subunits B1, B2, B3 and B4 is found at stations 16, 17–19, 20 and 21, respectively. The B5 subunit, with an intense pedogenic reddish color, only occurs SW of station 30, and between stations 17 and 20 on the NW wall. The thicker sector of the B1–B4 subunits may indicate the approximate location of the scarp toe (depositional axis) during the time they were deposited. The surface runoff flowing perpendicularly to the scarp would be concentrated and deflected along the base of the antislope scarp, eventually increasing its scouring capability. This evidence suggests that the sediment trap developed at the foot of the scarp might have migrated episodically some meters toward the SW, controlling the deposition of sedimentary bodies with an overall offlap arrangement. In fact, a 1-m thick sedimentary package deposited by a modern flow event would be restricted to the SW of station 25.

The wedge-shaped Unit C is a slope-wash massive sand and silt with scattered clasts, including a small gravel paleochannel that indicates a paleocurrent subparallel to the scarp. Two samples collected from this unit at a vertical distance of 38 cm have been dated at 19,021 ± 1,191 and 9,937 ± 656 OSL years BP (errors at 1σ). It has not been possible to elucidate whether this unit, devoid of stratigraphic markers, is deformed or not. Fault F8 seems to be onlapped by unit C, but its base is unclear, probably because the slope wash deposits of unit C are largely derived from reworking of unit B and thus have a similar composition. Unit D is a gravelly soil disturbed by ploughing. It locally fills artificial pits (locally known as *andalán*) excavated for the plantation of vines.

Structure

The overall structure exposed on the trench walls corresponds to graben and horst blocks NE of fault F6, and a double monocline SW of F6 whose upper and lower crests are truncated by normal and low-angle reverse faults, respectively (Fig. 6). According to McCalpin (1996), drape-type monoclinal folds associated with normal faults are particularly frequent in cohesive surficial deposits. An "articulated" monoclinal structure in volcanic tuffs has been described by McCalpin (2005) associated with the 50-m high scarp of the Pajarito normal fault in the Los Alamos National Laboratory area (Basin and Range, New Mexico). Probably, a relatively well-defined SW-dipping normal fault in the competent Paleozoic bedrock splays upward through the overlying alluvial cover (Rockwell and Ben-Zion 2007) forming the 25-m wide deformation zone observed in the trench (Fig. 7).

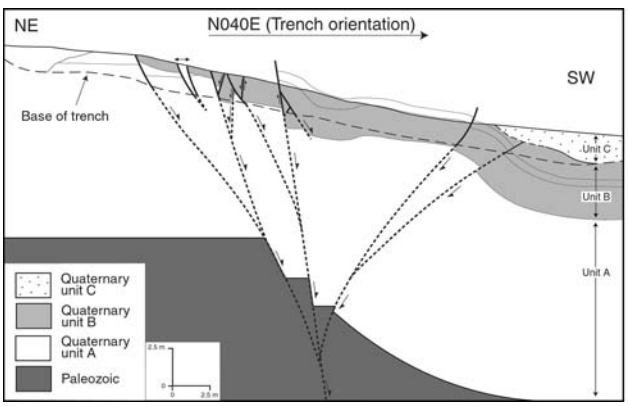

Fig. 7 Inferred geological cross-section of the trench area. The section assumes that Unit A is 12-m thick and that its thickness remains constant across the fault zone

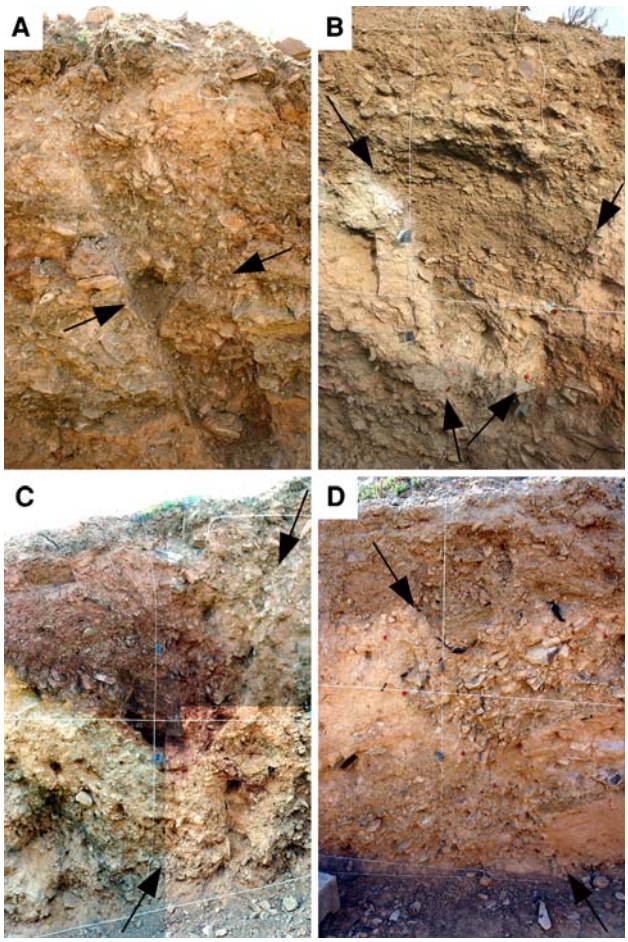

Fig. 8 Close-up views of some deformational structures exposed in the trench. **a** Fissure fill (between *arrows*) at station 12 of the SE wall of the trench. **b** Graben structure (between *arrows*) at station 14 of the SE wall. **c** Roll-over anticline at the upper crest of the monocline at station 17–18 of the NW wall (see Fig. 6). **d** Reverse fault (between *arrows*) in the lower crest of the monocline at station 31 of the NW wall

The structures exposed on the SE wall, and the main differences found on the opposite wall, are briefly explained below (Fig. 6). Fault F1, with a vertical offset of 95 cm, is defined by a tapering-downward shear zone up to 36-cm wide. Long-axes of the clasts are prevalently parallel to the fault zone. Sediments of A1 are horizontal in the footwall and back-tilted about 2° in the hanging wall. Between faults F1 and F2 there is a SW-dipping gravel-filled fissure generated by the outward rotation (about 2°) of the upper block (Fig. 8a). Toppling associated with the dilational opening of this fissure has produced an apparent down to the NE vertical separation of 9 cm. The fissure fill, up to 75-cm wide, shows a typical oriented fabric with the long axes of the clasts subparallel to the lower fissure wall (McCalpin 1996, pp. 118). Fault F2 and the antithetic fault F3 bound a wedge-shaped downdropped block (Fig. 8b). The block between faults F3 and F4 is a graben with internal deformation (drag folds). The high-angle fault F4 is cross-cut by the low-angle F5 fault, recording at least two faulting events subsequent to B3 subunit. The block between faults F4 and F6 corresponds to a horst truncated by fault F5. A cumulative vertical separation of 170 cm has been measured on faults F2 through F5.

The high-angle normal fault F6, which truncates the upper crest of the monocline, shows marked differences on both walls of the trench. On the SE wall, unit B on the downdropped block dips to the SW, whereas in the opposite wall it shows a roll-over anticline (Fig. 8c). Southwest of fault F6, we have mapped an antithetic failure plane that seems to be cross-cut by a low-angle synthetic fault.

The lower crest of the monocline is affected by two apparently reverse faults (F7 and F8) (Fig. 8d). Fault F7 on the SE wall is defined by a 35-cm wide reddish zone, and fault F8 has a relatively low dip ($\sim 30°$). These faults may correspond to oversteepened (refracted) normal faults which may have been rotated by the monoclinal flexure or which, conversely, may have controlled the development of the monocline. Such apparently reverse faults can form by coseismic normal faulting. For example, two normal fault earthquakes, the 1983 Borah Peak (M 6.9) and the 1959 Hegben Lake (M 7.3), produced small thrust fault ruptures several hundred meters long at the surface on the downthrown block (Myers and Hamilton 1964; Crone et al. 1987). Albeit reverse faults may also form at the toe of a rotational slide, we rule out this interpretation for F7 and F8, since these coarse-grained pediment deposits are not appropriate for the development of this type of mass movement, and because there is no geomorphic evidence of any landslide at the trench site. As indicated above, it has not been possible to prove that unit C is not affected by F8 fault, although this is our preferred interpretation.

The total cumulative vertical displacement directly measured in the trench (Fig. 6) is ca. 7.4 m ($95–9 + 170 + 240 + 30 + 160 + 50 = 736$ cm). This deformation, occurred subsequent to deposition of the material sampled in subunit A1 (ca. 72 ka), yields a vertical slip rate of 0.10 ± 0.01 mm/year (2σ error) for the Munébrega W Fault at the trench site. This is a minimum value, since we are using a maximum age for the deformation, and the trench probably did not expose all the vertical offset of unit A, as the interpretative cross-section of Fig. 7 suggests.

Contrary to what we expected, no coarse-grained colluvial wedges have been deposited in the antislope fault scarp zone. The reason for this is that normal faulting, rather than producing large free face scarps, has been accommodated by the formation of a monoclinal flexure and small surface ruptures (scarps and fissures) distributed throughout a broad deformation band. Similar structures are described by Pantosti et al. (1993) and McCalpin (2005). In our case, most of the scarp face corresponds to a dip slope underlain by a monocline. Additionally, the

episodic forward migration of the fault scarp has caused the incorporation of sedimentary units once deposited at the base of the scarp onto the upper erosional part of the scarp, probably reducing the potential of the site for capturing paleoseismic evidence.

Paleoseismic interpretation

A minimum of three faulting events are required to explain the stratigraphical and structural relationships exposed in the trench (Fig. 6). The first surface rupture event (event X) formed an antislope scarp, creating a sediment trap that confined deposition of unit B to the SW of fault F1. The base of B1 is a low-angle unconformity, which truncates layers of A1, and is interpreted as the event horizon X. Deposition and subsequent erosion of unit B (around 5-m thick) on the upthrown block northeast of fault F1 is ruled out simply because the antislope scarp isolates this relict sector of the mantled pediment from any runoff contributing area, thus precluding erosion. Event X occurred between 72 ka (deposition of subunit A1) and 41 ka (deposition of subunit B1). This event is probably much younger than 72 ka, since this age corresponds to an intermediate layer of A1. After deposition of this layer and before event X, the upper layers of A1 accumulated, a soil with a reddish Bt horizon developed, and the channeled subunit A2 formed, eroding the soil. Most likely F1 formed during event X before deposition of unit B. However, the fact that it sharply juxtaposes units A1 and B1 indicates that it has also moved after deposition of B1. It is probable that the topographic scarp created by event X was higher than 1.5 m, the minimum relief needed to block deposition of unit B1. This indicates that other structures in addition to fault F1, with a vertical offset of 95 cm (partially gained after deposition of B1), operated at event X.

Two subsequent faulting events (events Y and Z) are required to explain the cross-cutting relationship observed between faults F4 and F5 affecting unit B. Event Y formed the high-angle antithetic normal fault F4 and event Z produced the low-angle synthetic fault F5 that offsets the previous one (Fig. 6). Events Y and Z occurred sometime after deposition of subunit B3, that is, after 33 ka (age of unit B2) and possibly before 19 ka, the oldest age obtained for the presumably undeformed unit C. These are very probably the bracketing ages for the most recent event (MRE) recorded at the trench site.

The magnitude of the surface-rupturing paleoearthquakes that occurred on the Munébrega Faults can be estimated from the fault length using scaling relations (e.g., Wells and Coppersmith 1994; Stirling et al. 2002). We have not characterized single-event displacements in detail, so the more refined estimations based on them (Hemphill-Haley and Weldon 1999) cannot be done. Wells and Coppersmith (1994), using an extensive dataset, described that earthquake magnitude is proportional to the logarithm of the rupture length. Stirling et al. (2002) considerably expanded this dataset, and updated the magnitude-length regressions by Wells and Coppersmith (1994). They noted that the Wells and Coppersmith (1994) relationships underestimate the magnitude if the rupture length used was the fault trace length as mapped for preinstrumental ruptures. This underestimation is reasonable, since erosion tends to obliterate ancient earthquake ruptures, so the mapped rupture lengths are frequently smaller than the true ones. According to the regression for preinstrumental earthquakes proposed by Stirling et al. (2002) and assuming that morphogenic earthquakes ruptured the whole mapped length of the Munébrega W Fault (ca. 20 km), earthquakes with moment magnitudes of $M = 6.9$ (1σ error range 6.8–7.1) might be expected on this structure.

The three identified paleoearthquakes occurred over the past 72 ka yield a mean recurrence of ca. 24 ka. This could be considered as a maximum (optimistic) estimate due to the following reasons: (1) The age of the oldest event is very poorly constrained and could be considerably younger than 72 ka. (2) More than three earthquakes may have occurred on the Munébrega W Fault during the last 72 ka. The geometrical relationships of the trench do not allow us to establish an unambiguous relative chronology for most of the structures and consequently the inferred paleoseismic record may underrepresent the actual sequence of faulting events. On the other hand, a minimum of 7.4 m of cumulative vertical displacement close to the termination of the fault trace might be difficult to justify with only three paleoearthquakes, that is, a minimum average vertical offset per event of 2.5 m (assuming that all the deformation occurred coseismically). The empirical relationships presented by Wells and Coppersmith (1994) indicate that average displacements of 0.5 m (1σ error range of 0.3–0.9 m) might be expected in coseismic surface ruptures around 20-km long. However, regressions derived from preinstrumental earthquakes of Stirling et al. (2002), which provide higher estimates of coseismic surface displacements, yield a surface average displacement of 2.3 m (1σ range of 1.4–3.8 m) for surface ruptures 20-km long. A comparable average earthquake recurrence interval of 25–30 ka has been inferred from a paleoseismic investigation for the 24-km long El Camp normal Fault, also located in an intraplate orogen in the NE of Spain (Masana et al. 2001). The calculated vertical slip rate for that fault ranges from 0.02–0.08 mm/year (Masana et al. 2001; Perea et al. 2003).

Conclusions

The trench dug across the upslope-facing scarp produced by the Munébrega W Fault, across Upper Pleistocene

pediment deposits, demonstrates that this normal fault constitutes a seismogenic source capable of producing large surface-rupturing earthquakes.

A minimum of three faulting events during the past 72 ka has been inferred from the stratigraphical and geometrical relationships observed in the trench, yielding an average recurrence interval of 24 ka. This could be considered as a maximum or optimistic value, since the calculation has been derived from a maximum age for the oldest faulting event and the inferred paleoseismic record is likely incomplete. According to the obtained OSL dates, the most recent faulting event most likely occurred before 19 ka.

The cumulative vertical displacement measured on the trench (7.4 m) yields a minimum vertical slip rate of the fault at the trench site of 0.10 mm/year subsequent to 72 ka.

According to the regressions for preinstrumental earthquakes proposed by Stirling et al. (2002), earthquakes with moment magnitudes of $M \approx 6.9$ might be expected on this structure with a mappable length of ca. 20 km.

At the trenching site, surface ruptures on this fault have not produced the typical large and well-defined free-face scarps with colluvial wedges, but rather a wide surface rupture zone with small normal-fault scarplets and fissures in the upper part of the scarp, and a monoclinal flexure in the lower part. The scarp face migrated episodically toward the downthrown block, incorporating into the upper erosional part of the scarp sedimentary units originally deposited on the downthrown block.

A minimum age of 8 ka has been obtained for the most recent event on the Munébrega E Fault, dating an undeformed pediment deposit that overlies unconformably this structure. The Quaternary activity of this fault is strongly suggested but not demonstrated.

The largest earthquake magnitude historically recorded in the Iberian Range is 5.7, but paleoseismic events probably had magnitudes up to ca. 7 (Gutiérrez et al. 2008 and this work). Thus, the available probabilistic seismic hazard analyses, solely based on historical and instrumental data, may underestimate the probability of occurrence of large, damaging earthquakes. There is a need to conduct further paleoseismological investigations on the already known Quaternary faults in order to evaluate and improve the predictive capability of the existing probabilistic seismic hazard analyses in this range.

Acknowledgments The authors are very grateful to Mr. Santiago Galve for giving permission to dig the trench in his property, and to Dr. Juan Herrero for helping in the interpretation of the soil horizons exposed in the trench walls. Excellent and thorough reviews by Dr. Kris Vanneste and Dr. José J. Martínez-Díaz substantially improved the original version of the manuscript. FG forms part of the consolidated research group "Geomorphology and Global Change-E68" of the Aragón Government. This work has been co-financed by the Spanish Education and Science Ministry and the FEDER (project CGL2007–60766) as well as by the Aragón Government (PM008/2007).

References

Adrover R, Feist M, Hugueney M, Mein P, Moissenet E (1982) L'âge et la mise en relief de la formation détritique culminante de la Sierra Pelarda (prov. de Teruel, Espagne). C R Acad Sci Paris 295(II):231–236

Alfaro JA, Casas AM, Simón JL (1987) Ensayo de zonación sismotectónica en la Cordillera Ibérica, Depresión del Ebro y borde Sur Pirenaico. Estudios Geológicos 43:445–457

Anadón P, Roca E (1996) Geological setting of the Tertiary basins of Northeast Spain. In: Friend P, Dabrio CJ (eds) Tertiary basins of Spain, the stratigraphic record of crustal kinematics. Cambridge University Press, Cambridge, pp 43–48

Andeweg B (2002) Cenozoic tectonic evolution of the Iberian Peninsula. Causes and effects of changing stress fields. Dissertation, Vrije Universiteit, Amsterdam, pp 1–178

Baena J, Moreno F, Nozal F, Alfaro JA, Barranco L (1992) Mapa Neotectónico y Sismotectónico de España a escala 1:1,000,000. IGME/ENRESA. Unpublished

Blair TC, Mcpherson JG (1994) Alluvial fans and their natural distinction from rivers based on morphology, hydraulic processes, sedimentary processes, and facies assemblages. J Sediment Res A64(3):450–489

Bomer B (1960) Aspectos morfológicos de la Cuenca de Calatayud-Daroca y de sus zonas marginales. Estud Geogr 80:393–402

Burbank DW, Anderson RS (2001) Tectonic geomorphology. Blackwell, Massachussets, pp 1–274

Burillo F, Gutiérrez M, Peña JL (1985) Datación arqueológica de deformaciones tectónicas en vertientes holocenas de Sierra Palomera (Cordillera Ibérica centroriental) Actas da I Reunião do Quaternário Ibérico. Lisboa 2:355–366

Capote R, Muñoz JA, Simón JL, Liesa CL, Arlegui LE (2002) Alpine tectonics I: the Alpine system north of the Betic Cordillera. In: Gibbons W, Moreno T (eds) The Geology of Spain. The Geological Society, London, pp 367–400

Cendrero A (2003) De la comprensión de la historia de la Tierra al análisis y predicción de las interacciones entre seres humanos y medio natural. Discurso de recepción. Real Academia de Ciencias Exactas, Físicas y Naturales, Madrid, pp 1–60

Crone AH, Machette MN, Bonilla MG, Lienkaemper JJ, Pierce KL, Scott WE, Bucknam RC (1987) Surface faulting accompanying the Borah Peak earthquake and segmentation of the Lost River fault, central Idaho. Bull Seismol Soc Am 77:739–770

del Olmo P, Hernández A, Aragonés E (1983) Mapa Geológico de España, E. 1:50,000. Ateca (437). Instituto Geológico y Minero de España (I.G.M.E.) Madrid. pp 67 + map

Echeverría M (1988) Geomorfología de la rama aragonesa de la Cordillera Ibérica entre las depresiones de Calatayud y Almazán y su reborde soriano. Dissertation, Universidad de Zaragoza, pp 1–969

European Macroseismic Scale (1998) Cahiers du Centre Europeen de Geodynamique et de Seismologie 15:1–99

García-Mayordomo J, Faccioli E, Paolucci R (2004) Comparative study of the seismic hazard assessments in European national seismic codes. Bull Earthquake Eng 2(1):51–73

Giardini D, Jiménez MJ, Grünthal G (2003) European-Mediterranean Seismic Hazard Map. European Seismological Commission. http://wija.ija.csic.es/gt/earthquakes/

Gutiérrez F (1996) Gypsum karstification induced subsidence: effects on alluvial systems and derived geohazards (Calatayud Graben, Iberian Range, Spain). Geomorphology 16:277–293

Gutiérrez F (1998) Fenómenos de subsidencia por disolución de formaciones evaporíticas en las fosas neógenas de Teruel y Calatayud. Dissertation, University of Zaragoza, pp 1–569

Gutiérrez F, Gracia FJ, Gutiérrez M (1996) Consideraciones sobre el final del relleno endorreico de las fosas de Calatayud y Teruel y su paso al exorreismo. Implicaciones morfo-estratigráficas y estructurales. Cadernos do Laboratorio Xeolóxico de Laxe 21:23–43

Gutiérrez F, Gracia J, Gutiérrez M (2005) Karst, neotectonics and periglacial features in the Iberian Range. In: Desir G, Gutiérrez F, Gutiérrez M (eds) Sixth international conference on geomorphology, field trip guides 2:343–400

Gutiérrez F, Gutiérrez M, Gracia FJ, McCalpin JP, Lucha P, Guerrero J (2008) Plio-Quaternary extensional seismotectonics and drainage network development in the central sector of the Iberian Range (NE Spain). Geomorphology. doi:10.1016/j.geomorph.2007.07.020

Hemphill-Haley MA, Weldon II RJ (1999) Estimating prehistoric earthquake magnitude from point measurements of surface rupture. Bull Seismol Soc Am 89(5):1264–1279

Henares J, López-Casado C, Sanz de Galdeano C, Delgado J, Peláez JA (2003) Stress fields in the Iberian-Maghrebi region. J Seismol 7(1):65–78

Herraiz M, De Vicente G, Lindo-Ñaupari R, Giner J, Simón JL, González-Casado JM, Vadillo O, Rodríguez-Pascua MA, Cicuéndez JI, Casas A, Cabañas L, Rincón P, Cortés AL, Ramírez M, Lucini M (2000) The recent (upper Miocene to Quaternary) and present tectonic stress distributions in the Iberian Peninsula. Tectonics 19(4):762–786

Instituto Geográfico Nacional (2007) Catálogo de sismos próximos. http://www.ign.es/ign/es/IGN/SisCatalogo.jsp

Jabaloy A, Galindo-Zaldívar J, González-Lodeiro F (2002) Palaeostress evolution of the Iberian Peninsula (late Carboniferous to present-day). Tectonophysics 357(1–4):159–186

Jiménez MJ, García-Fernández M, The GSHAP Ibero-Maghreb Working Group (1999) Seismic hazard assessment in the Ibero-Maghreb region. Ann Geofis 42(6):1057–1065

Jiménez MJ, Giardini D, Grünthal G, SESAME Working Group (2001) Unified seismic hazard modelling throughout the Mediterranean Region. Boll Geofis Teorica Appl 42(1–2):3–18

Jiménez MJ, Giardini D, Grünthal G (2003) The ESC-SESAME Unified Hazard Model for the European-Mediterranean region. Centre Sismologique Euro-Méditerranéen/European-Mediterranean Seismological Centre (CSEM/EMSC) Newsletter 19:2–4

Leeder MR, Jackson JA (1993) The interaction between normal faulting and drainage in active extensional basins, with examples from the western United States and central Greece. Basin Res 10:7–18

Machette MN (1985) Calcic soils of the southwestern United States. In: Weide DL (ed) Quaternary soils and geomorphology of the american southwest. Geological Society of America, Special Paper 203, pp 1–21

Martín-Serrano A (ed) (2005) Mapa geomorfológico de España y del margen continental escala 1:1,000,000. Instituto Geológico y Minero de España, Madrid, pp 1–232 + 2 maps

Martínez-Solares JM, Mezcua J (2002) Catálogo sísmico de la Península Ibérica (880 a.C.–1900). Monografía 18, Instituto Geográfico Nacional, Madrid, pp 1–253

Masana E, Villamarín JA, Sánchez-Cabañero J, Plaza J, Santanach P (2001) Seismogenic faulting in an area of low seismic activity: paleoseismicity of the El Camp fault (Northeast Spain). Geol Mijnbouw 80(3–4):229–241

McCalpin JP (1996) Paleoseismology in extensional tectonic environments. In: McCalpin JP (ed) Paleoseismology. Academic Press, San Diego, pp 85–146

McCalpin JP (2005) Late Quaternary activity of the Pajarito fault, Rio Grande rift of northern New Mexico, USA. Tectonophysics 408:213–236

Mezcua J (1982) Catálogo general de isosistas de la Península Ibérica. Instituto Geográfico Nacional, Madrid, pp 1–59 + 261 maps

Ministerio de Fomento (2002) Real Decreto 997/2002, de 27 de septiembre, por el que se aprueba la norma de construcción sismorresistente: parte general y edificación (NCSR-02). Boletín Oficial del Estado, 11 October, pp 35898–35967

Ministerio de Fomento (2003) Norma de construcción sismorresistente: parte general y edificación (NCSR-02). Con comentarios de la Subcomisión Permanente de Normas Sismorresistentes. Centro de Publicaciones del Ministerio de Fomento, Madrid (Spain), pp 1–94

Ministerio del Interior (2004) Resolución de 17 de septiembre de 2004, de la Subsecretaría, por la que se ordena la publicación del Acuerdo del Consejo de Ministros, de 16 de julio de 2004, por el que se modifica la Directriz básica de planificación de protección civil ante el riesgo sísmico, aprobada por el Acuerdo del Consejo de Ministros, de 7 de abril de 1995. Boletín Oficial del Estado, 2 October, pp 33205–33208

Myers WB, Hamilton W (1964) Deformation accompanying the Hebgen lake earthquake of August 17, 1959. U.S. Geological Survey Professional Paper 435, pp 55–98

Olaiz A, De Vicente G, Muñoz Martín A, Vegas R (2006) Mapa de esfuerzos de Europa a partir de mecanismos focales calculados desde el tensor de momento sísmico. Geogaceta 40:55–58

Pantosti D, Schwartz DP, Valensise G (1993) Paleoseismology along the 1980 surface rupture of the Irpina fault; implications for earthquake recurrence in the southern Apennines, Italy. J Geophys Res 98:6561–6577

Perea H, Figueiredo PM, Carner J, Gambini S, Boydell K (2003) Paleoseismological data from a new trench across the El Camp Fault (Catalan Coastal Ranges, NE Iberian Peninsula). Ann Geophys 46(5):763–774

Reiter L (1990) Earthquake hazard analysis; issues and insights. Columbia University Press, New York, pp 1–254

Reiter L (1995) Paleoseismology—a user's perspective. In: Serva L, Slemmons DB (eds) Perspectives in Paleoseismology. Association of Engineering Geologists Special Publication, vol 6, pp 3–6

Rey Pastor A, Bonelli J (1957) El sismo de Daroca-Used del 28 de Septiembre de 1953 y su relación con la línea sismotectónica del Jiloca. Instituto Geográfico Catastral, pp 1–16

Rockwell TK, Ben-Zion Y (2007) High localization of primary slip zones in large earthquakes from paleoseismic trenches: observations and implications for earthquake physics. J Geophys Res 112:B10304

Samardjieva E, Payo G, Badal J (1999) Magnitude formulae and intensity-magnitude relations for early instrumental earthquakes in the Iberian Region. Nat Hazards 19(2–3):189–204

Simón JL (1989) Late Cenozoic stress field and fracturing in the Iberian Chain and Ebro Basin (Spain). J Struct Geol 11:285–294

Sopeña A, Gutiérrez-Marco JC, Sánchez-Moya Y, Gómez JJ, Mas R, García A, Lago M (Coords.) (2004) Cordilleras Ibérica y Costero Catalana. In: Vera JA (ed) Geología de España. IGME, Madrid, pp. 467–470

Stirling M, Rhoades D, Berryman K (2002) Comparison of earthquake scaling relations derived from data of the instrumental and preinstrumental era. Bull Seismol Soc Am 92(2):812–830

Tena JM, Mandado JA (1984) Estudio geológico de la Cuenca terciaria de Calatayud-Daroca. Rev Acad Cienc Zaragoza 39:69–78

Wells DL, Coppersmith KJ (1994) New empirical relationships among magnitude, rupture length, rupture width, rupture area, and surface displacement. Bull Seismol Soc Am 84(4):974–1002